



## Research article

# Finite-time trajectory tracking control for a 12-rotor unmanned aerial vehicle with input saturation

Chunyang Fu<sup>a</sup>, Yantao Tian<sup>a,b,\*</sup>, Haiyang Huang<sup>a</sup>, Lei Zhang<sup>a</sup>, Cheng Peng<sup>c</sup>

<sup>a</sup> College of Communication Engineering, Jilin University, Changchun, 130025, PR China

<sup>b</sup> Key Laboratory of Bionic Engineering of Ministry of Education, Jilin University, Changchun, 130025, PR China

<sup>c</sup> Changchun Institute of Optics Fine Mechanics and Physics, Chinese Academy of Sciences, Changchun, 130000, PR China



## ARTICLE INFO

## Keywords:

Unmanned aerial vehicle  
Finite-time control  
Input saturation  
Finite-time auxiliary system  
Finite-time stability

## ABSTRACT

Finite-time trajectory tracking problem for a novel 12-rotor unmanned aerial vehicle (UAV) with input saturation is investigated in this paper. The UAV is divided into outer loop (altitude system and translational system) and inner loop (attitude system), and hierarchical structure is adopted to design the control scheme. In order to ensure finite-time convergence property and compensate input saturation impact simultaneously, a finite-time backstepping control strategy combined with a finite-time auxiliary system is proposed for the outer loop. Additional signals are generated to prevent control performance degradation caused by input saturation. The finite-time stability for outer loop is rigorously proved via Lyapunov theory. For inner loop, linear active disturbance rejection control is employed for attitude controllers design to enhance the robustness against the lumped disturbances. Finally simulation experiments illustrate the effectiveness and superiority of the proposed algorithm.

## 1. Introduction

Multi-rotor unmanned aerial vehicles (MUAVs) have been widely used in various military and civilian fields owing to the excellent properties such as vertical take-off and landing (VTOL), hovering and load carrying capacity, high agility and maneuverability. Autonomous navigation and control of the MUAVs are very important for different flight missions, for example, search and rescue in hazardous environment, surveillance, inspection and mapping. However, the coupling, model uncertainty and delay existing in the MUAV as well as the external disturbances acting on the MUAV make the flight control system design a more challenging work. Actuator saturation problem also limits and degrades the effectiveness of the flight controller. In order to increase the dynamic response speed and enhance the tracking performance under input saturation and total disturbances, finite-time trajectory tracking control for a 12-rotor unmanned aerial vehicle (UAV) is investigated in this paper to lay a good foundation for the autonomous flight.

In recent years, many efforts have been made to deal with the trajectory tracking problem for MUAVs. Various control methods such as linear quadratic regulator (LQR) [1], proportional–integral–derivative (PID) control [2], sliding mode control [3], intelligent control [4–6],

robust control [7], disturbance-observer-based control [8] and backstepping control [9] are used in the controller design of MUAVs. Among them, recursive backstepping offers a systematic framework based on Lyapunov theory for design of tracking and regulation strategies. Command filtered backstepping fault-tolerance control was designed for small UAVs in Ref. [10]. Integral backstepping sliding mode control was proposed in Ref. [11] and adaptive backstepping was developed in Ref. [12] to tackle trajectory tracking problem for quadrotors under external disturbances. A backstepping tracking controller was formulated for a quadrotor to track a moving ground target in Ref. [13]. Nonlinear backstepping trajectory tracking control for quadrotor UAVs was developed based on nonlinear disturbance observer in Ref. [14]. In above literatures, backstepping-based controllers gained good tracking performance for MUAVs. However, only asymptotic stability was guaranteed for the closed-loop system, which means the tracking errors will converge to zero when time approaches to infinite. For the sake of increasing convergence rate of the tracking errors and meeting high real-time requirement of the MUAV when executing flight missions, finite-time control strategy needs to be introduced into backstepping to ensure the finite-time stability of the closed-loop system.

Finite-time control strategy provides faster convergence rate, higher precision control performance, and better disturbance rejection

\* Corresponding author. College of Communication Engineering, Jilin University, Changchun, 130025, PR China.

E-mail addresses: [fucy15@mails.jlu.edu.cn](mailto:fucy15@mails.jlu.edu.cn) (C. Fu), [tianty@jlu.edu.cn](mailto:tianty@jlu.edu.cn) (Y. Tian), [huanghy0424@qq.com](mailto:huanghy0424@qq.com) (H. Huang), [591607360@qq.com](mailto:591607360@qq.com) (L. Zhang), [litianjinorc@126.com](mailto:litianjinorc@126.com) (C. Peng).

<https://doi.org/10.1016/j.isatra.2018.08.005>

Received 6 March 2018; Received in revised form 21 June 2018; Accepted 5 August 2018

Available online 10 August 2018

0019-0578/© 2018 ISA. Published by Elsevier Ltd. All rights reserved.

property, so as to improve the dynamic as well as steady-state performance and guarantee the finite-time stability of the closed-loop system [15]. Finite-time control based on homogenous theory was proposed for quadrotors to achieve hovering in Ref. [16] and trajectory tracking in Ref. [17]. Global fast dynamic terminal sliding mode control was employed to tackle finite-time position tracking problem for quadrotors in Ref. [18]. Adaptive sliding mode control with an adaptive-tuning scheme was developed for finite-time stabilization of UAVs under uncertainties in Ref. [19]. In above literatures, finite-time controllers were designed based on homogenous theory or sliding mode control method. However, homogenous approach cannot adjust or even estimate the settling time with complicated stability analysis process, and chattering phenomenon in sliding mode control needs to be taken into account [15,20]. Compared with above, finite-time backstepping strategy is a much simpler and easier control method with finite-time convergence property. Moreover, none of the above literatures considered input saturation problem for MUAVs, which would limit and degrade the effectiveness of the flight controller.

Input saturation exists in MUAV system due to rotor speed limitation. Thrust force saturation has immense effect on performance degradation since the control law would act unexpectedly with saturation. When model uncertainties and external disturbances acting on MUAVs simultaneously, the input saturation problem is more likely to appear. Hence, taking into account input saturation problem is necessary for the flight control system design. Structured anti-windup compensators were applied to quadrotor UAVs in Ref. [21]. An emendatory tracking error was introduced to prevent system performance from degradation due to actuator saturation in Ref. [22]. A model reference adaptive control with integral state feedback combined with a modern anti-windup compensator was presented for an autonomous underwater vehicle under input saturation in paper [23]. Nested saturation controllers were designed for outer loop of the quadrotor to guarantee asymptotic stability in Ref. [24]. A new variable structure and variable coefficient PID anti-windup control was proposed as the yaw controller to prevent actuator saturation of an eight-rotor UAV in Ref. [25]. In above literatures, only asymptotic stability was gained when considering input saturation problem for MUAVs. Ensuring finite-time convergence property and compensating input saturation effect simultaneously for MUAVs under external disturbances make the flight control system design a more complicated situation.

To sum up, finite-time trajectory tracking control for a 12-rotor UAV under input saturation is investigated in this paper. The 12-rotor UAV is divided into inner loop and outer loop, and hierarchical control structure is adopted to design the control scheme. In order to obtain finite-time convergence property and compensate input saturation impact of the outer loop, a finite-time backstepping control strategy combined with finite-time auxiliary system is proposed. Since good regulation performance for attitude system plays a very important role in accurate trajectory tracking task, linear active disturbance rejection control (LADRC) is introduced for inner loop due to its strong robustness against the lumped disturbance including coupling, model uncertainty and external disturbance.

The main contributions of this paper mainly lie in the outer loop control of the 12-rotor UAV: (1) Finite-time trajectory tracking problem for a novel 12-rotor UAV under input saturation and external disturbances is considered in this paper. (2) In order to ensure finite-time convergence property and compensate input saturation impact simultaneously for outer loop of the UAV, a finite-time backstepping control strategy combined with a finite-time auxiliary system is proposed. (3) The outer loop gains faster convergence rate, higher precision control performance, and better disturbance rejection property under the finite-time backstepping controller. (4) Additional signals are generated by the finite-time auxiliary system to attenuate input saturation impact. Controller parameter selection range is also relaxed due to the auxiliary system, which further enhances the robustness of the outer loop. (5) Finite-time stability of the closed-loop system under

the proposed controller is rigorously proved by Lyapunov theory.

The outline of this paper is as follow: the next section presents the problem formulation and preliminaries. In section 3, the whole flight control scheme design for the 12-rotor UAV is investigated. In section 4, simulation experiments are carried out to show the strong robustness and good tracking performance for the UAV under our proposed controller. Finally, the conclusions of this work are given in the last section.

**Notations:** The variables appearing in this paper are defined as follow:  $E = \{O_g, x_g, y_g, z_g\}$  is the earth-fixed inertial frame,  $B = \{O_b, x_b, y_b, z_b\}$  is the body-fixed frame. The state variables of the UAV include absolute position of the center of mass  $\zeta = [x, y, z]^T$  in frame  $E$  (where  $x$  and  $y$  are translational motions,  $z$  is altitude motion), attitude motion  $\eta = [\phi, \theta, \psi]^T$  in frame  $E$  (where  $\phi$  is roll angle,  $\theta$  is pitch angle,  $\psi$  is yaw angle), linear velocity  $V = [u, v, w]^T$  and angular velocity  $\Omega = [p, q, r]^T$  in frame  $B$ . Matrix  $T$  is the angular velocity transformation matrix and matrix  $R$  is the linear velocity transformation matrix between frame  $E$  and frame  $B$ . The inputs of the UAV are  $F$  and  $\tau = [\tau_\phi, \tau_\theta, \tau_\psi]^T$ , where  $F$  is the thrust force and  $\tau = [\tau_\phi, \tau_\theta, \tau_\psi]^T$  is the torque generated by the rotors. Other physical parameters of the UAV like  $m$  is the mass,  $J = \text{diag}(I_x, I_y, I_z)$  is the moment of inertia matrix, where  $I_x$  is the moment of inertia along  $x$  direction,  $I_y$  along  $y$  direction and  $I_z$  along  $z$  direction.  $[\Delta I_x, \Delta I_y, \Delta I_z]^T$  is the parameter uncertainty of attitude system.  $g$  is gravitational acceleration,  $e_3 = [0, 0, 1]^T$  is the unit vector of  $z$  direction.  $[d_x, d_y, d_z]^T$  represents the external disturbances acting on each channel of the outer loop,  $[D_x, D_y, D_z]^T$  is the upper bounds of the disturbances in outer loop,  $[d_\phi, d_\theta, d_\psi]^T$  denotes the external disturbances acting on attitude channels,  $[D_\phi, D_\theta, D_\psi]^T$  is the upper bounds of the disturbances in attitude channels.  $x_d, y_d, z_d$  are desired trajectories for each channel of the outer loop,  $\phi_d, \theta_d, \psi_d$  are desired attitude angles for each channel of the inner loop. In this paper, we introduced auxiliary system to tackle the input saturation problem,  $\xi_1$  and  $\xi_2$  are state variables, and  $c_1, c_2, \nu$  are parameters of the auxiliary system. The rest of the parameters in this paper are controller parameters need to be designed.

## 2. Problem formulation and preliminaries

The 12-rotor UAV investigated in this paper has a coaxial structure with twelve rotors. The scheme is shown in Fig. 1. Twelve rotors are installed in pairs at the end of the connecting rod to provide the power for various flying missions.

Literatures [26–28] describe the specific modeling process of the 12-rotor UAV, and here we simply give the main result of the modeling. The angular velocity relationship matrix  $T$  and linear velocity relationship matrix  $B$  between frame  $E$  and frame  $B$  are

$$T = \begin{bmatrix} 1 & s_\phi t_\theta & c_\phi t_\theta \\ 0 & c_\phi & -s_\phi \\ 0 & s_\phi/c_\theta & c_\phi/c_\theta \end{bmatrix} \quad (1)$$

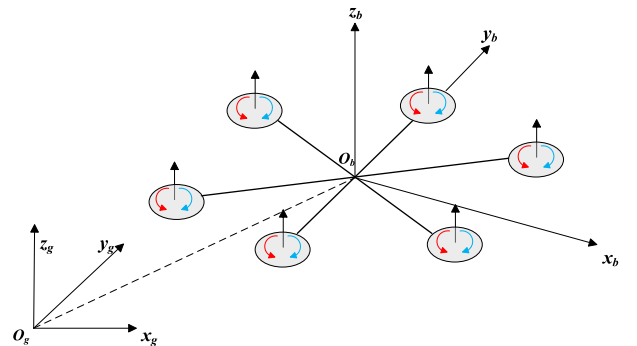


Fig. 1. The scheme of the 12-rotor UAV.

$$R = \begin{bmatrix} c_\psi c_\theta & c_\psi s_\theta s_\phi - s_\psi c_\phi & c_\psi s_\theta c_\phi + s_\psi s_\phi \\ s_\psi c_\theta & s_\psi s_\theta s_\phi + c_\psi c_\phi & s_\psi s_\theta c_\phi - c_\psi s_\phi \\ -s_\theta & c_\theta s_\phi & c_\theta c_\phi \end{bmatrix} \quad (2)$$

where  $s_\phi = \sin \phi$ ,  $c_\phi = \cos \phi$ ,  $t_\theta = \tan \theta$ .

According to Newton-Euler equation, the dynamic model of the 12-rotor UAV is derived as

$$\begin{cases} \dot{\zeta} = RV \\ \dot{V} = -ge_3 + \frac{F}{m}R^T e_3 \\ \dot{\eta} = T\Omega \\ J\dot{\Omega} = -\Omega \times J\Omega + \tau \end{cases} \quad (3)$$

On the basis of model (3), considering external disturbances acting on each channel, the model for outer loop of the UAV is

$$\begin{cases} \ddot{x} = \frac{F}{m} \cos \phi \sin \theta \cos \psi + \sin \phi \sin \psi + d_x \\ \ddot{y} = \frac{F}{m} \cos \phi \sin \theta \sin \psi - \sin \phi \cos \psi + d_y \\ \ddot{z} = \frac{F}{m} \cos \phi \cos \theta - g + d_z \end{cases} \quad (4)$$

The model for inner loop of the UAV is

$$\begin{cases} \ddot{\phi} = -\frac{I_z - I_y}{I_x} qr + \frac{\tau_\phi}{I_x} + d_\phi \\ \ddot{\theta} = -\frac{I_x - I_z}{I_y} pr + \frac{\tau_\theta}{I_y} + d_\theta \\ \ddot{\psi} = -\frac{I_y - I_x}{I_z} pq + \frac{\tau_\psi}{I_z} + d_\psi \end{cases} \quad (5)$$

The 12-rotor UAV is a typical underactuated system moving with six degrees of freedom  $x, y, z, \phi, \theta, \psi$ , but only four degrees of freedom  $z, \phi, \theta, \psi$  can be controlled independently by four control inputs  $F$  and  $\tau = [\tau_\phi, \tau_\theta, \tau_\psi]^T$ .

The control objective of this paper is to force the 12-rotor UAV tracking the desired trajectory  $x_d, y_d, z_d$  in finite time under input saturation and external disturbances.

**Assumption 1.** All state signals  $\zeta, \eta, \dot{\zeta}, \dot{\eta}$  are measurable by on-board sensors.

**Assumption 2.** Roll angle and pitch angle are assumed to satisfy the following inequalities  $-\pi/2 \leq \phi \leq \pi/2$ ,  $-\pi/2 \leq \theta \leq \pi/2$ .

**Assumption 3.** The reference trajectories and their first and second derivatives are continuous and assumed to be bounded.

**Assumption 4.** The external disturbance has upper bound  $d_j \leq D_j$ ,  $j = x, y, z, \phi, \theta, \psi$ , where  $D_j$  is a known constant.

**Lemma 1.** [29]. Consider the following system

$$\dot{x} = f(x), \quad f(0) = 0, \quad x \in \mathbb{R}^n$$

For any real number  $\gamma > 0$ ,  $\beta > 0$ ,  $0 < \iota < 1$ , there exists a continuous positive definite function  $V: \mathbb{R}^n \rightarrow \mathbb{R}$  satisfying

$$\dot{V}(x) + \gamma V(x) + \beta V^\iota(x) \leq 0$$

the equilibrium of the system is finite-time stable and the settling time satisfies

$$T \leq \frac{1}{\gamma(1-\iota)} \ln \frac{\gamma V^{1-\iota}(x_0) + \beta}{\beta}$$

### 3. Control scheme design

This section presents the whole control scheme design for the 12-rotor UAV as shown in Fig. 2. Finite-time backstepping controllers are designed for outer loop (altitude channel and translational channels) to track the desired references  $x_d, y_d, z_d$  in finite time. A finite-time

auxiliary system is added into altitude channel to compensate the unexpected action caused by input saturation in thrust force. LADRC attitude controllers are used to generate control torques in order to balance out the coupling, model uncertainty and external disturbance in the attitude system.

#### 3.1. Altitude control

Considering input saturation, the altitude dynamics described in (4) is given as

$$\begin{cases} \dot{z}_1 = z_2 \\ \dot{z}_2 = u_s \cos \phi \cos \theta / m - g + d_z \end{cases} \quad (6)$$

where  $[z_1, z_2]^T = [z, \dot{z}]^T$  is the vector of state variables in altitude channel.  $u_s$  denotes the plant input subject to saturation type non-linearity described as

$$u_s = \begin{cases} u_{\max}, & u > u_{\max} \\ u, & u_{\min} \leq u \leq u_{\max} \\ u_{\min}, & u < u_{\min} \end{cases} \quad (7)$$

where  $u$  is the ideal control action,  $u_{\max}$  and  $u_{\min}$  are the upper bound and lower bound of the input saturation constraint.

A finite-time backstepping controller combined with a finite-time auxiliary system is designed for altitude system to track the desired vertical reference  $z_d$  and compensate the input saturation impact in finite time.

##### Step 1

Define compensation errors as

$$e_1 = z_1 - z_d - \xi_1, \quad e_2 = z_2 - \alpha - \xi_2 \quad (8)$$

where  $\xi_1$  and  $\xi_2$  are the states of the finite-time auxiliary system

$$\begin{cases} \dot{\xi}_1 = -\xi_1 - c_1 |\xi_1|^\nu \operatorname{sgn}(\xi_1) + \xi_2 \\ \dot{\xi}_2 = -\xi_2 - c_2 |\xi_2|^\nu \operatorname{sgn}(\xi_2) + (u_s - u) \cos \theta \cos \phi / m \end{cases} \quad (9)$$

where  $c_1 > 0$ ,  $c_2 > 0$ ,  $0 < \nu < 1$  are positive constants.

Select the Lyapunov candidate as

$$V_1 = \frac{1}{2} e_1^2 \quad (10)$$

Take the derivative of  $V_1$ , we get

$$\begin{aligned} \dot{V}_1 &= e_1 \dot{e}_1 \\ &= e_1 (e_2 + \alpha + \xi_2 - \dot{z}_d + \dot{\xi}_1 + c_1 |\xi_1|^\nu \operatorname{sgn}(\xi_1) - \dot{\xi}_2) \\ &= e_1 (e_2 + \alpha + \xi_2 + c_1 |\xi_1|^\nu \operatorname{sgn}(\xi_1) - \dot{z}_d) \end{aligned} \quad (11)$$

Then design the virtual control function as

$$\alpha = -k_1 e_1 - l_1 |e_1|^\sigma \operatorname{sgn}(e_1) - \xi_1 - c_1 |\xi_1|^\nu \operatorname{sgn}(\xi_1) + \dot{z}_d \quad (12)$$

where  $k_1 > 0$ ,  $l_1 > 0$ ,  $0 < \sigma < 1$  are positive constants.

Substitute (12) into (11),

$$\dot{V}_1 = -k_1 e_1^2 - l_1 |e_1|^{\sigma+1} + e_1 e_2 \quad (13)$$

##### Step 2

Select the Lyapunov candidate as

$$V_2 = \frac{1}{2} e_2^2 \quad (14)$$

Take the derivative of  $V_2$ , we get

$$\begin{aligned} \dot{V}_2 &= e_2 \dot{e}_2 \\ &= e_2 (u \cos \phi \cos \theta / m - g + d_z - \dot{\alpha} + \dot{\xi}_2 + c_2 |\xi_2|^\nu \operatorname{sgn}(\xi_2)) \end{aligned} \quad (15)$$

Design the ideal control action as

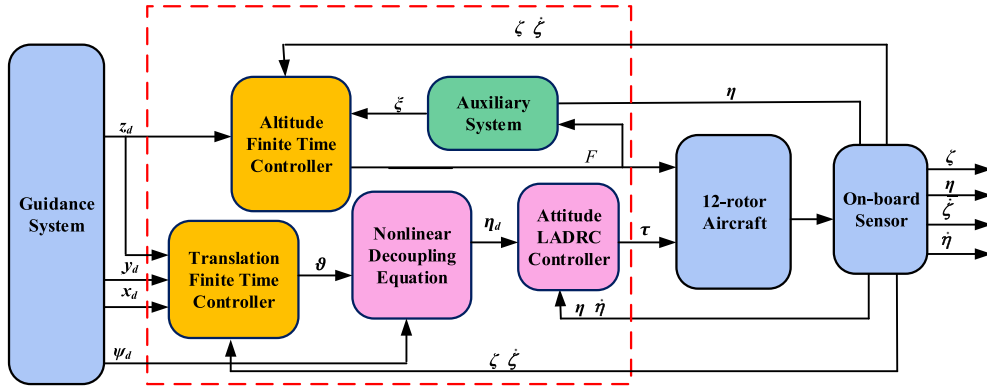


Fig. 2. Control scheme of the 12-rotor UAV.

$$u = m(-k_2 e_2 - l_2 |e_2|^\sigma \text{sgn}(e_2) + g + \dot{\alpha}) / \cos \theta \cos \phi - m(\xi_2 + c_2 |\xi_2|^\rho \text{sgn}(\xi_2) + e_1) / \cos \theta \cos \phi \quad (16)$$

where  $k_2 > 0$ ,  $l_2 > 0$ ,  $0 < \sigma < 1$  are positive constants, and  $\dot{\alpha} = \frac{\partial \alpha}{\partial z_1} \dot{z}_1 + \frac{\partial \alpha}{\partial z_2} \dot{z}_2 + \frac{\partial \alpha}{\partial z_d} \dot{z}_d + \frac{\partial \alpha}{\partial \phi} \dot{\phi}$ . Substitute (16) into (15),

$$\dot{V}_2 = -k_2 e_2^2 - l_2 |e_2|^{\sigma+1} - e_1 e_2 + e_2 d_z \quad (17)$$

**Theorem 1.** Consider altitude dynamics (6) in the presence of input saturation and external disturbance, suppose Assumptions 1–4 are satisfied, the finite-time auxiliary system is constructed as (9), under virtual control (12) and ideal control (16), the state trajectory of altitude system can converge to the desired trajectory in finite time.

**Proof.** Select the whole Lyapunov function as

$$V = V_1 + V_2 \quad (18)$$

Take the derivative of  $V$ , we can get

$$\begin{aligned} \dot{V} &= -k_1 e_1^2 - l_1 |e_1|^{\sigma+1} + e_1 e_2 - k_2 e_2^2 - l_2 |e_2|^{\sigma+1} - e_1 e_2 + e_2 d_z \\ &= -k_1 e_1^2 - l_1 |e_1|^{\sigma+1} - k_2 e_2^2 - l_2 |e_2|^{\sigma+1} + e_2 d_z \\ &\leq -k_1 e_1^2 - l_1 |e_1|^{\sigma+1} - k_2 e_2^2 - l_2 |e_2|^{\sigma+1} + |e_2| D_z \\ &= -k_1 e_1^2 - l_1 |e_1|^{\sigma+1} - k_2 e_2^2 - \left(l_2 - \frac{D_z}{|e_2|^\sigma}\right) |e_2|^{\sigma+1} \end{aligned} \quad (19)$$

Define  $\gamma_1 = 2k_1$ ,  $\gamma_2 = 2k_2$ ,  $\beta_1 = 2^{\frac{\sigma+1}{2}} l_1$ ,  $\beta_2 = 2^{\frac{\sigma+1}{2}} \left(l_2 - \frac{D_z}{|e_2|^\sigma}\right)$ , the derivative of  $V$  is rewritten as

$$\begin{aligned} \dot{V} &\leq -\gamma_1 \left(\frac{e_1^2}{2}\right) - \gamma_2 \left(\frac{e_2^2}{2}\right) - \beta_1 \left(\frac{e_1^2}{2}\right)^{\frac{\sigma+1}{2}} - \beta_2 \left(\frac{e_2^2}{2}\right)^{\frac{\sigma+1}{2}} \\ &\leq -\gamma V - \beta V^\iota \end{aligned} \quad (20)$$

where  $\gamma = \min\{\gamma_1, \gamma_2\}$ ,  $\beta = \min\{\beta_1, \beta_2\}$ ,  $\iota = (\sigma + 1)/2$ .

Since  $0 < \sigma < 1$ ,  $0.5 < \iota < 1$  is derived, which meets the requirement of Lemma 1. Let  $|e_2| \geq (D_z/l_2)^{1/\sigma}$ , then  $\beta_2 > 0$ , and  $\dot{V}$  is negative definite. According to Lemma 1, the state trajectory of altitude system converges to the desired trajectory in finite-time. And error  $e_2$  converges to the region  $\Xi_z$  in finite time.

$$|e_2| \leq \Xi_z \leq \left(\frac{D_z}{l_2}\right)^{\frac{1}{\sigma}} \quad (21)$$

This concludes the proof.

The whole design process of altitude controller is shown in Algorithm 1 and Algorithm 2.

Algorithm 1

Altitude controller design process.

---

**Input:** desired trajectory  $z_d$ , altitude states  $z_1, z_2$ , auxiliary states  $\xi_1, \xi_2$ , attitude angles  $\phi, \theta$   
**Output:** ideal control action  $u$

---

- 1: calculate compensation error in step 1:  $e_1 = z_1 - z_d - \xi_1$
  - 2: obtain virtual control function:  
 $\alpha = -k_1 e_1 - l_1 |e_1|^\sigma \text{sgn}(e_1) - \xi_1 - c_1 |\xi_1|^\rho \text{sgn}(\xi_1) + \dot{z}_d$
  - 3: calculate compensation error in step 2:  $e_2 = z_2 - \alpha - \xi_2$
  - 4: obtain ideal control action:  
 $u = m(-k_2 e_2 - l_2 |e_2|^\sigma \text{sgn}(e_2) + g + \dot{\alpha}) / \cos \theta \cos \phi - m(\xi_2 + c_2 |\xi_2|^\rho \text{sgn}(\xi_2) + e_1) / \cos \theta \cos \phi$
- 

Algorithm 2

Finite-time auxiliary system design process.

---

**Input:** attitude angles  $\phi, \theta$ , ideal control action  $u$   
**Output:** auxiliary states  $\xi_1, \xi_2$

---

- 1: calculate  $\dot{\xi}_1 = -\xi_1 - c_1 |\xi_1|^\rho \text{sgn}(\xi_1) + \xi_2$
  - 2: calculate  $\dot{\xi}_2 = -\xi_2 - c_2 |\xi_2|^\rho \text{sgn}(\xi_2) + (u_s - u) \cos \theta \cos \phi / m$
- 

**Remark 1.** The region  $\Xi_z$  can be guaranteed small enough if  $D_z/l_2 < 1$ . Since  $1/\sigma > 1$ ,  $\Xi_z$  will be greatly reduced by the exponential term. Therefore, the parameter  $l_2$  needs to meet the condition as  $l_2 > D_z$ .

**Remark 2.** According to (21), bigger  $l_2$  will make the boundary  $\Xi_z$  smaller, which is beneficial to attain faster convergence rate, higher tracking precision and stronger robustness. However, bigger  $l_2$  also generates greater control action and leads to input saturation problem more easily. The above contradiction can be alleviated through compensating the input saturation effect by the finite-time auxiliary system in our algorithm. The control parameter selections are relaxed, and the tradeoff between convergence rate and actuator saturation is avoided to a certain extent.

### 3.2. Translational control

Desired translational references tracking is achieved through attitude variation. Hence, finite-time backstepping virtual controllers are designed for translational system so as to derive the desired attitude angles for inner loop. In order to facilitate controller design process, we define desired trajectory as  $[x_d, y_d, z_d]^T = [\Upsilon_1, \Upsilon_2, \Upsilon_3]^T$ , external disturbance  $[d_x, d_y, d_z]^T = [d_1, d_2, d_3]^T$ ,  $[\vartheta_1, \vartheta_2, \vartheta_3]^T = [\ddot{x}, \ddot{y}, \ddot{z}]^T$  is the virtual control vector needs to be designed, and let  $i = 1, 2, 3$ .

**Table 1**  
Physical parameter of the 12-rotor UAV.

Parameter	Value
$m$	2.5 kg
$I_x$	$8.1 \times 10^{-3} \text{ Nms}^{-2}$
$I_y$	$8.1 \times 10^{-3} \text{ Nms}^{-2}$
$I_z$	$14.2 \times 10^{-3} \text{ Nms}^{-2}$

### Step 1

Define the tracking errors as

$$[\chi_{11}, \chi_{12}, \chi_{13}]^T = [x - Y_1, y - Y_2, z - Y_3]^T \quad (22)$$

$$[\chi_{21}, \chi_{22}, \chi_{23}]^T = [\dot{x} - \alpha_1, \dot{y} - \alpha_2, \dot{z} - \alpha_3]^T \quad (23)$$

where  $[\alpha_1, \alpha_2, \alpha_3]^T$  is the intermediate control vector needs to be designed.

Select the Lyapunov candidate as

$$V_{1i} = \frac{1}{2} \chi_{1i}^2 \quad (24)$$

Take the derivative of  $V_{1i}$ , we get

$$\dot{V}_{1i} = \chi_{1i} \dot{\chi}_{1i} = \chi_{1i} (\chi_{2i} + \alpha_i - Y_i) \quad (25)$$

The intermediate control function is designed as

$$\alpha_i = -\delta_{1i} \chi_{1i} - \lambda_{1i} |\chi_{1i}|^{\mu_i} \text{sgn}(\chi_{1i}) + Y_i \quad (26)$$

where  $\delta_{1i} > 0$ ,  $\lambda_{1i} > 0$ ,  $0 < \mu_i < 1$  are positive constants.

Substitute (26) into (25),

$$\dot{V}_{1i} = -\delta_{1i} \chi_{1i}^2 - \lambda_{1i} |\chi_{1i}|^{\mu_i+1} + \chi_{1i} \chi_{2i} \quad (27)$$

### Step 2

Select the Lyapunov candidate as

$$V_{2i} = \frac{1}{2} \chi_{2i}^2 \quad (28)$$

Take the derivative of  $V_{2i}$ , we get

$$\dot{V}_{2i} = \chi_{2i} \dot{\chi}_{2i} = \chi_{2i} (\vartheta_i - \dot{\alpha}_i + d_i) \quad (29)$$

The virtual control action is designed as

$$\vartheta_i = -\delta_{2i} \chi_{2i} - \lambda_{2i} |\chi_{2i}|^{\mu_i} \text{sgn} |\chi_{2i}| + \dot{\alpha}_i - \chi_{1i} \quad (30)$$

where  $\delta_{2i} > 0$ ,  $\lambda_{2i} > 0$ ,  $0 < \mu_i < 1$  are positive constants.

Substitute (30) into (29),

$$\dot{V}_{2i} = -\delta_{2i} \chi_{2i}^2 - \lambda_{2i} |\chi_{2i}|^{\mu_i+1} - \chi_{1i} \chi_{2i} + \chi_{2i} d_i \quad (31)$$

**Theorem 2.** Consider outer loop dynamics (4), suppose Assumptions 1–4 are satisfied, under intermediate control function (26) and virtual control action (30), the tracking errors of translational system converge to the origin in finite time.

**Proof.** Select the whole Lyapunov function as

$$V_i = V_{1i} + V_{2i} \quad (32)$$

Take the derivative of  $V_i$ , we get

$$\begin{aligned} \dot{V}_i &= -\delta_{1i} \chi_{1i}^2 - \lambda_{1i} |\chi_{1i}|^{\mu_i+1} + \chi_{1i} \chi_{2i} - \delta_{2i} \chi_{2i}^2 - \lambda_{2i} |\chi_{2i}|^{\mu_i+1} - \chi_{1i} \chi_{2i} + \chi_{2i} d_i \\ &\leq -\delta_{1i} \chi_{1i}^2 - \lambda_{1i} |\chi_{1i}|^{\mu_i+1} - \delta_{2i} \chi_{2i}^2 - \lambda_{2i} |\chi_{2i}|^{\mu_i+1} + |\chi_{2i}| |D_i| \\ &\leq -\delta_{1i} \chi_{1i}^2 - \lambda_{1i} |\chi_{1i}|^{\mu_i+1} - \delta_{2i} \chi_{2i}^2 - \left( \lambda_{2i} - \frac{D_i}{|\chi_{2i}|^{\mu_i}} \right) |\chi_{2i}|^{\mu_i+1} \\ &\leq -2\delta_{1i} \left( \frac{\chi_{1i}^2}{2} \right) - 2\delta_{2i} \left( \frac{\chi_{2i}^2}{2} \right) - 2^{\frac{\mu_i+1}{2}} \lambda_{1i} \left( \frac{\chi_{1i}^2}{2} \right)^{\frac{\mu_i+1}{2}} \\ &\quad - 2^{\frac{\mu_i+1}{2}} \left( \lambda_{2i} - \frac{D_i}{|\chi_{2i}|^{\mu_i}} \right) \left( \frac{\chi_{2i}^2}{2} \right)^{\frac{\mu_i+1}{2}} \end{aligned} \quad (33)$$

Define

$$\delta_i = \min\{2\delta_{1i}, 2\delta_{2i}\}, \lambda_i = \min\left\{2^{\frac{\mu_i+1}{2}} \lambda_{1i}, 2^{\frac{\mu_i+1}{2}} \left( \lambda_{2i} - \frac{D_i}{|\chi_{2i}|^{\mu_i}} \right)\right\}, \omega_i = \frac{\mu_i+1}{2},$$

the derivative of  $V_i$  is rewritten as

$$\dot{V}_i \leq -\delta_i V_i - \lambda_i V_i^{\omega_i} \quad (34)$$

Since  $0 < \mu_i < 1$ ,  $0.5 < \omega_i < 1$  is derived. Let  $|\chi_{2i}| \geq (D_i/\lambda_{2i})^{1/\mu_i}$ , then  $\lambda_i > 0$ , and  $\dot{V}_i$  is negative definite. According to Lemma 1, the state trajectories of translational system converge to the desired trajectories in finite-time. The tracking error  $\chi_{2i}$  converges to the region  $\Delta_i$  in finite time

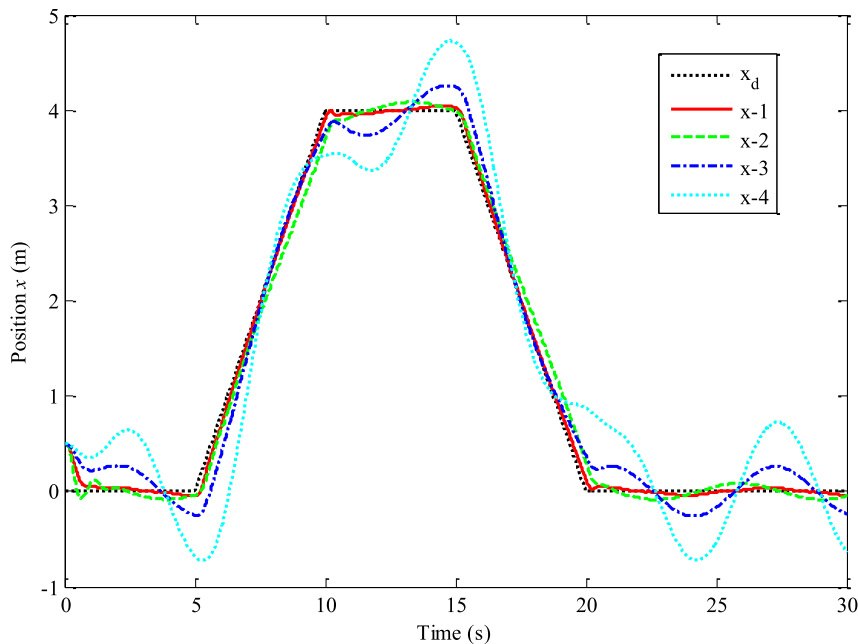


Fig. 3. Tracking result of position  $x$ .

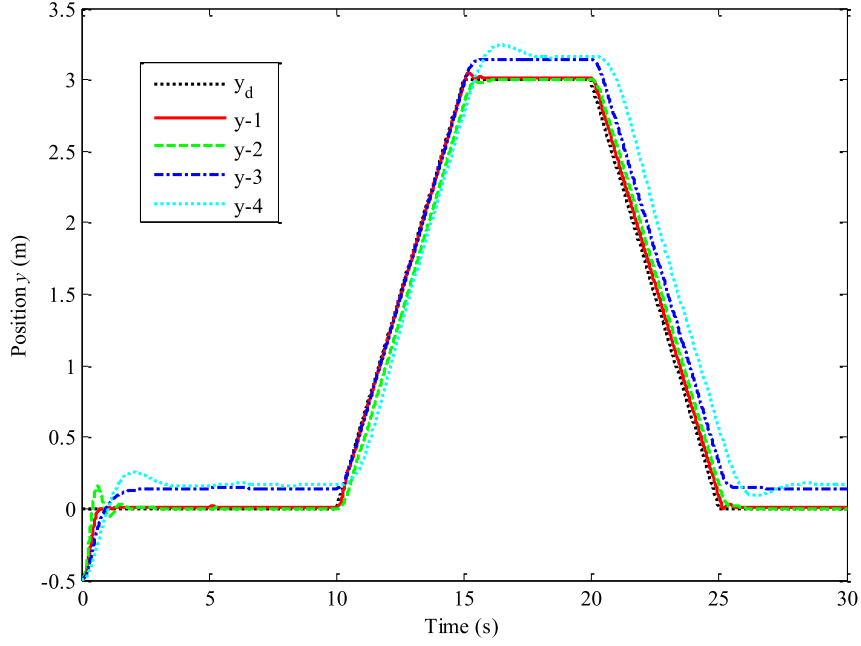


Fig. 4. Tracking result of position y.

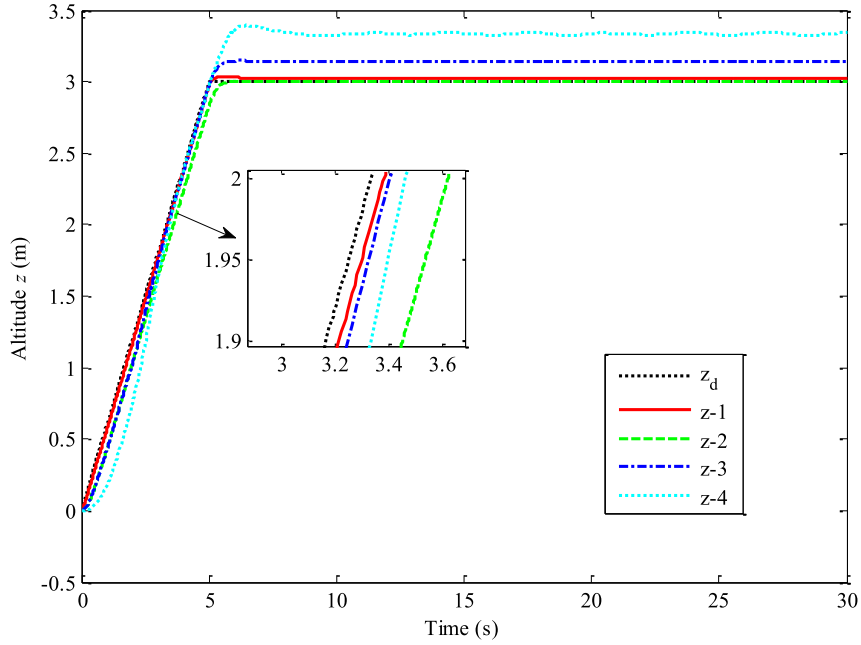


Fig. 5. Tracking result of position z.

$$|\kappa_{2i}| \leq \Delta_i \leq \left(\frac{D_i}{\lambda_{2i}}\right)^{\frac{1}{\mu_i}} \quad (35)$$

This concludes the proof.

The whole design process of translational controller is shown in Algorithm 3.

**Algorithm 3**

Translational controller design process.

**Input:** desired trajectory  $[x_d, y_d, z_d]^T = [\Upsilon_1, \Upsilon_2, \Upsilon_3]^T$ , position  $x, y, z$ , velocity  $\dot{x}, \dot{y}, \dot{z}$

**Algorithm 3 (continued)**

**Output:** desired attitude angles  $\phi_d, \theta_d$

- 1: calculate tracking error in step
  - 1:  $\chi_{11} = x - \Upsilon_1, \chi_{12} = y - \Upsilon_2, \chi_{13} = z - \Upsilon_3$ ,
- 2: obtain intermediate control function:
 
$$\alpha_i = -\delta_{1i}\chi_{1i} - \lambda_{1i} |\chi_{1i}|^{\mu_i} \text{sgn}(\chi_{1i}) + \dot{\Upsilon}_i$$
- 3: calculate tracking error in step
  - 2:  $\chi_{21} = \dot{x} - \alpha_1, \chi_{22} = \dot{y} - \alpha_2, \chi_{23} = \dot{z} - \alpha_3$
- 4: obtain virtual control action:
 
$$\vartheta_i = -\delta_{2i}\chi_{2i} - \lambda_{2i} |\chi_{2i}|^{\mu_i} \text{sgn} |\chi_{2i}| + \dot{\alpha}_i - \chi_{1i}$$

(continued on next page)

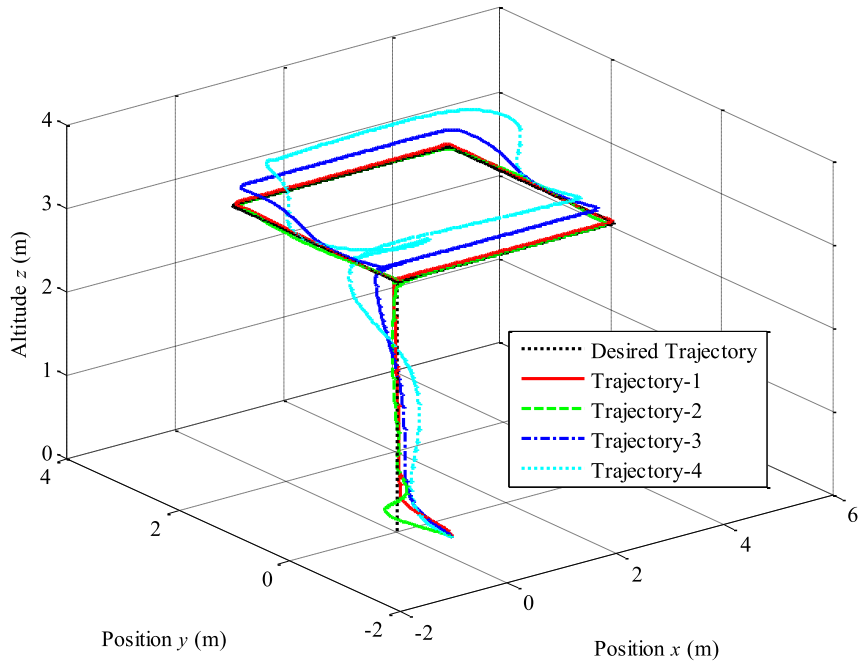


Fig. 6. Three-dimensional tracking result.

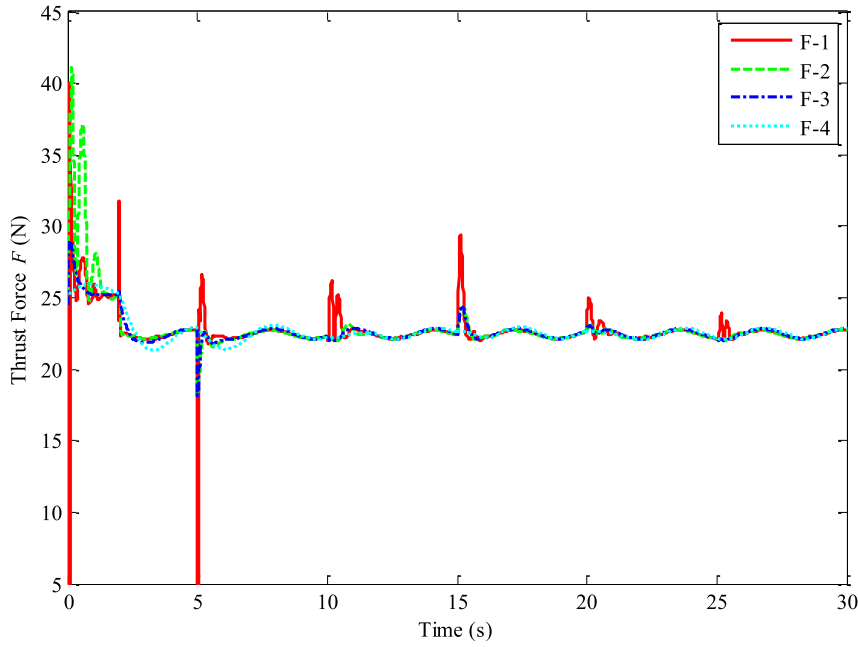


Fig. 7. Curves of thrust force.

Algorithm 3 (continued)

- 
- 5: calculate desired roll angle:  $\phi_d = \arcsin\left(\frac{\vartheta_1 \sin \psi - \vartheta_2 \cos \psi}{\sqrt{\vartheta_1^2 + \vartheta_2^2 + (\vartheta_3 + g)^2}}\right)$
  - 6: calculate desired pitch angle:  $\theta_d = \arctan\left(\frac{\vartheta_1 \cos \psi + \vartheta_2 \sin \psi}{\vartheta_3 + g}\right)$
- 

**Remark 3.** The region  $\Delta_i$  can be guaranteed small enough if  $D_i/\lambda_{2i} < 1$ . Since  $1/\mu_i > 1$ , the  $\Delta_i$  will be greatly reduced by the exponential term. Therefore, the parameter  $\lambda_{2i}$  needs to meet the condition as  $\lambda_{2i} > D_i$ .

According to the nominal outer loop dynamics (4) without disturbances, we can get the following formulas by doing some simple

calculations

$$\vartheta_1 \cos \theta \cos \psi + \vartheta_2 \cos \theta \sin \psi - (\vartheta_3 + g) \sin \theta = 0 \quad (36)$$

$$\begin{aligned} \vartheta_1(\sin \theta \cos \psi \sin \phi - \sin \psi \cos \phi) + \vartheta_2(\sin \theta \sin \psi \sin \phi + \cos \psi \cos \phi) \\ + (\vartheta_3 + g) \cos \theta \sin \phi = 0 \end{aligned} \quad (37)$$

$$\begin{aligned} \vartheta_1(\sin \theta \cos \psi \cos \phi + \sin \psi \sin \phi) + \vartheta_2(\sin \theta \sin \psi \cos \phi - \cos \psi \sin \phi) \\ + (\vartheta_3 + g) \cos \theta \sin \phi = \frac{F}{m} \end{aligned} \quad (38)$$

In actual flight, attitude angles are always adjusting to maintain the stability of the UAV, therefore we assume the pitch angle is not equal to zero. Divide equation (36) by  $\cos \theta$  on both sides, we get the desired pitch angle for inner loop as

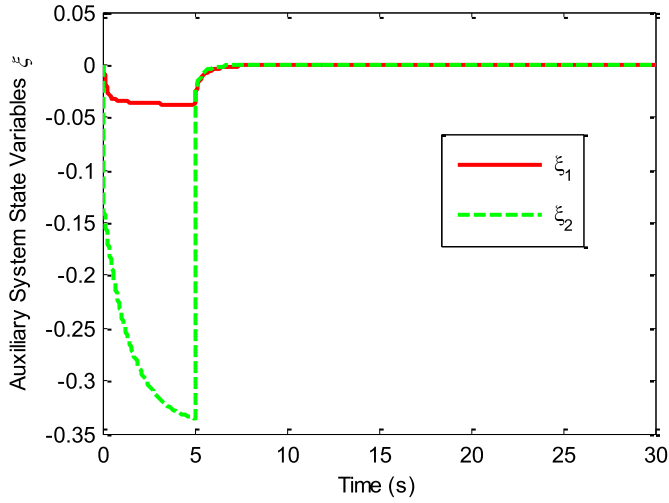


Fig. 8. States of finite-time auxiliary system.

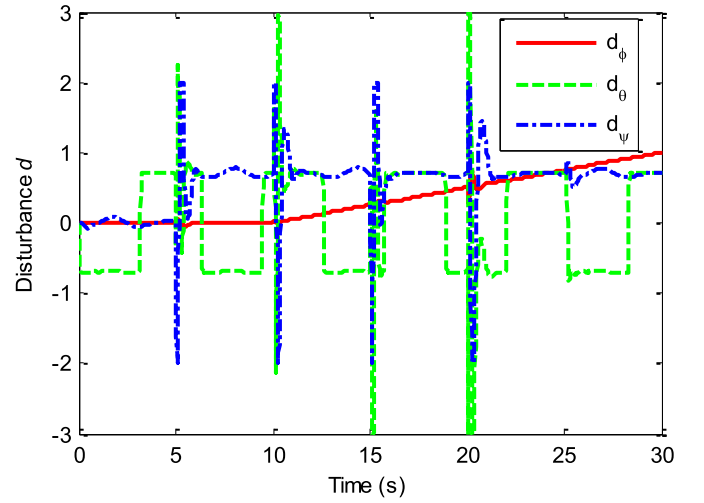


Fig. 10. Lumped disturbance estimation result.

$$\theta_d = \arctan\left(\frac{\partial_1 \cos \psi + \partial_2 \sin \psi}{\partial_3 + g}\right) \quad (39)$$

According to (37) and (38), the desired roll angle for inner loop is derived as

$$\phi_d = \arcsin\left(\frac{\partial_1 \sin \psi - \partial_2 \cos \psi}{\sqrt{\partial_1^2 + \partial_2^2 + (\partial_3 + g)^2}}\right) \quad (40)$$

### 3.3. Attitude control

Good regulation performance of attitude system plays a very important role for trajectory tracking tasks. For the sake of achieving high precision control performance of the attitude system under coupling, model uncertainty and external disturbance, LADRC is introduced to design the attitude controllers due to its strong robustness. Based on the online estimation of the above total disturbances by linear extended state observer (LESO), the controller is able to counteract all factors affecting the control precision, which lays a good foundation for trajectory tracking task.

Table 2

Integral square error of position states for 12-rotor UAV.

ISE	$e_x$	$e_y$	$e_z$
Approach1	0.1586	0.1095	0.0147
Approach2	0.6232	0.3451	0.1401
Approach3	1.3956	0.9543	0.5707
Approach4	8.7602	2.6136	3.1903

The attitude system described in (5) is rewritten as the second order system with respect to parameter uncertainty as follow

$$\begin{cases} \dot{\zeta}_{i1} = \zeta_{i2} \\ \dot{\zeta}_{i2} = b_i \tau_i + \tau_{id} \end{cases} \quad i = 1, 2, 3 \quad (41)$$

where  $\zeta_{i1} = [\phi, \theta, \psi]^T$  and  $\zeta_{i2} = [\dot{\phi}, \dot{\theta}, \dot{\psi}]^T$  are state variables, control torque  $\tau_i = [\tau_\phi, \tau_\theta, \tau_\psi]^T$  is the input of the attitude system,  $b_i = [1/I_x, 1/I_y, 1/I_z]^T$  is the nominal value of the moment of inertia,  $[\Delta I_x, \Delta I_y, \Delta I_z]^T$  is the parameter uncertainty,  $\tau_{id}$  is the lumped disturbance including coupling, parameter uncertainty and external

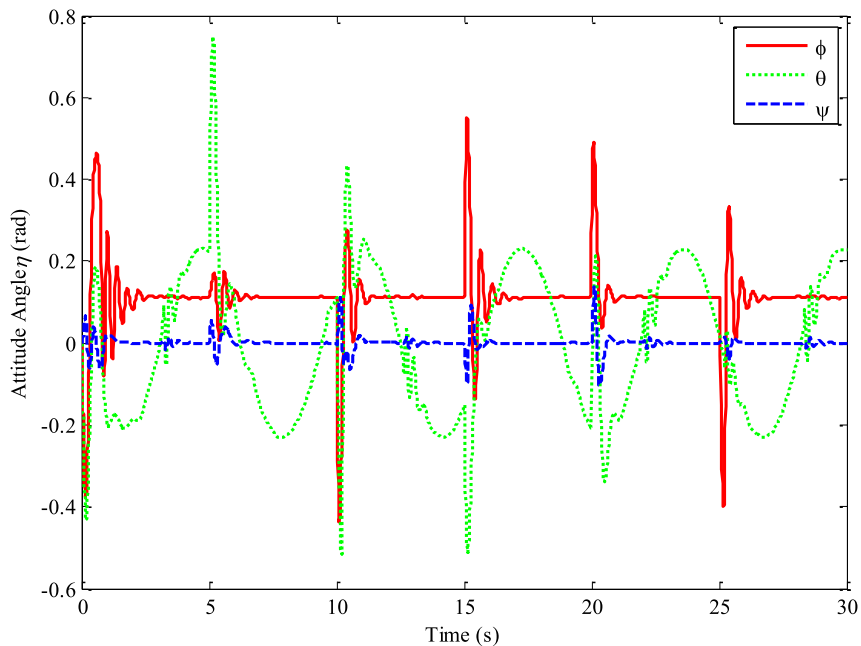


Fig. 9. Attitude system regulation result.

disturbance as  $\tau_{id} = -((I_z + \Delta I_z) - (I_y + \Delta I_y))qr/(I_x + \Delta I_x) - \Delta I_x \tau_\phi / I_x (I_x + \Delta I_x) + d_\phi$ ,  
 $\tau_{2d} = -((I_x + \Delta I_x) - (I_z + \Delta I_z))pr/(I_y + \Delta I_y) - \Delta I_y \tau_\theta / I_y (I_y + \Delta I_y) + d_\theta$ ,  
 and  $\tau_{3d} = -((I_y + \Delta I_y) - (I_x + \Delta I_x))pq/(I_z + \Delta I_z) - \Delta I_z \tau_\psi / I_z (I_z + \Delta I_z) + d_\psi$ .

The specific design process of the controllers is as follow

Extend system (41) into a third order system as

$$\begin{cases} \dot{\zeta}_{i1} = \zeta_{i2} \\ \dot{\zeta}_{i2} = b_i \tau_i + \zeta_{i3} \quad i = 1, 2, 3 \\ \dot{\zeta}_{i3} = \hat{h}_i(\zeta_i, \tau_{id}) \end{cases} \quad (42)$$

where  $\zeta_{i3} = \tau_{id}$  is the extended state variable.

The LESO is designed for system (42), with  $\varepsilon_{i1} = \zeta_{i1} - \hat{\zeta}_{i1}$  being the estimation error

$$\begin{cases} \dot{\hat{\zeta}}_{i1} = \hat{\zeta}_{i2} + \kappa_{i1} \varepsilon_{i1} \\ \dot{\hat{\zeta}}_{i2} = \hat{\zeta}_{i3} + b_i \tau_i + \kappa_{i2} \varepsilon_{i1} \\ \dot{\hat{\zeta}}_{i3} = \kappa_{i3} \varepsilon_{i1} \end{cases} \quad (43)$$

where  $\hat{\zeta}_{i1}$ ,  $\hat{\zeta}_{i2}$ ,  $\hat{\zeta}_{i3}$  are the estimations of  $\zeta_{i1}$ ,  $\zeta_{i2}$ ,  $\tau_{id}$  respectively.  $\kappa_{i1} > 0$ ,  $\kappa_{i2} > 0$ ,  $\kappa_{i3} > 0$  are observer gains.

Define  $\zeta_{id} = [\phi_d, \theta_d, \psi_d]^T$  as the desired attitude trajectory, on the basis of observer (43), a linear feedback controller for attitude system is designed as

$$\tau_i = \frac{\lambda_{i1}(\zeta_{id} - \hat{\zeta}_{i1}) + \lambda_{i2}(\dot{\zeta}_{id} - \dot{\hat{\zeta}}_{i2}) + (\ddot{\zeta}_{id} - \ddot{\hat{\zeta}}_{i3})}{b_i} \quad (44)$$

where  $\lambda_{i1} > 0$ ,  $\lambda_{i2} > 0$  are controller gains.

Let (42) subtract (43), we get

$$\dot{\zeta}_i - \dot{\hat{\zeta}}_i = \begin{pmatrix} 0 & 1 & 0 \\ 0 & 0 & 1 \\ 0 & 0 & 0 \end{pmatrix} - \begin{pmatrix} \kappa_{i1} & 0 & 0 \\ \kappa_{i2} & 0 & 0 \\ \kappa_{i3} & 0 & 0 \end{pmatrix} (\zeta_i - \hat{\zeta}_i) + \begin{pmatrix} 0 \\ 0 \\ 1 \end{pmatrix} (\hat{h}_i(\zeta_i, \tau_{id}) - \hat{h}_i(\hat{\zeta}_i, \tau_{id})) \quad (45)$$

where  $\zeta_i = [\zeta_{i1}, \zeta_{i2}, \zeta_{i3}]^T$  and  $\hat{\zeta}_i = [\hat{\zeta}_{i1}, \hat{\zeta}_{i2}, \hat{\zeta}_{i3}]^T$ .

Calculate the characteristic polynomial for (45), and suppose that

$$\left| v_i I_3 - \begin{bmatrix} -\kappa_{i1} & 1 & 0 \\ -\kappa_{i2} & 0 & 1 \\ -\kappa_{i3} & 0 & 0 \end{bmatrix} \right| = v_i^3 + \kappa_{i1} v_i^2 + \kappa_{i2} v_i + \kappa_{i3} = (v_i + \varpi_i)^3 \quad (46)$$

where  $\varpi_i > 0$  is a positive constant.

The observer gains can be chosen in accordance with the following rules

$$\kappa_{ij} = \frac{3! \varpi_i^j}{j!(3-j)!}, \quad j = 1, 2, 3 \quad (47)$$

That is,

$$\kappa_i = [\kappa_{i1}, \kappa_{i2}, \kappa_{i3}]^T = [3\varpi_i, 3\varpi_i^2, \varpi_i^3]^T \quad (48)$$

The controller gains are always selected as

$$[\lambda_{i1}, \lambda_{i2}]^T = [\varpi_{ic}^2, 2\varpi_{ic}]^T, \quad \varpi_i = 3\varpi_{ic} \quad (49)$$

Substitute (48) into (45),

$$\dot{\mathfrak{N}}_i = \varpi_i A_i \mathfrak{N}_i + B_i \frac{\hat{h}_i(\zeta_i, \tau_{id}) - \hat{h}_i(\hat{\zeta}_i, \tau_{id})}{\varpi_i^3} \quad (50)$$

where  $\mathfrak{N}_i = [\mathfrak{N}_{i1}, \mathfrak{N}_{i2}, \mathfrak{N}_{i3}]^T = \left[ \frac{\zeta_{i1} - \hat{\zeta}_{i1}}{\varpi_i^0}, \frac{\zeta_{i2} - \hat{\zeta}_{i2}}{\varpi_i^1}, \frac{\zeta_{i3} - \hat{\zeta}_{i3}}{\varpi_i^2} \right]^T$ ,  $A_i = \begin{bmatrix} -3 & 1 & 0 \\ -3 & 0 & 1 \\ -1 & 0 & 0 \end{bmatrix}$ ,

$$B_i = \begin{bmatrix} 0 \\ 0 \\ 1 \end{bmatrix}$$

**Assumption 5.** Suppose  $\hat{h}_i(\zeta_i, \tau_{id})$  is global Lipschitz with  $\zeta_i$ , for any  $\hat{\zeta}_i$ , there exists a positive constant  $\rho_i$  satisfying the following inequality.

$$|\hat{h}_i(\zeta_i, \tau_{id}) - \hat{h}_i(\hat{\zeta}_i, \tau_{id})| \leq \rho_i \|\zeta_i - \hat{\zeta}_i\|$$

**Theorem 3.** Consider the attitude system (41), suppose Assumption 5 is satisfied, the linear extended state observer is constructed as (43), with the observer gains as (48), if the parameter  $\varpi_i$  is large enough to let

$$\lim_{t \rightarrow \infty} \mathfrak{N}_{ij}(t) = 0, \quad i = j = 1, 2, 3 \quad (51)$$

The estimation error of the extended state observer is asymptotically convergent.

**Theorem 4.** Consider the attitude system (41), suppose Assumptions 1–5 are satisfied, under the linear extended state observer (43) and the feedback controller (44), the attitude states are bounded.

**Proof.** Define attitude tracking errors as  $s_{i1} = \zeta_{id} - \zeta_{i1}$ ,  $s_{i2} = \dot{\zeta}_{id} - \dot{\zeta}_{i2}$ , then  $s_i = [s_{i1}, s_{i2}]^T$ . Define estimation errors of the observer as  $\varepsilon_{i1} = \zeta_{i1} - \hat{\zeta}_{i1}$ ,  $\varepsilon_{i2} = \zeta_{i2} - \hat{\zeta}_{i2}$ ,  $\varepsilon_{i3} = \zeta_{i3} - \hat{\zeta}_{i3}$ , then  $\varepsilon_i = [\varepsilon_{i1}, \varepsilon_{i2}, \varepsilon_{i3}]^T$ .

Substitute (43) and (44) into (41), we get

$$\dot{s}_i = F_i s_i + H_i \varepsilon_i \quad (52)$$

$$\text{where } F_i = \begin{bmatrix} 0 & 1 \\ -\lambda_{i1} & -\lambda_{i2} \end{bmatrix}, \quad H_i = \begin{bmatrix} 0 & 0 & 0 \\ -\lambda_{i1} & -\lambda_{i2} & -1 \end{bmatrix}.$$

This concludes the proof.

The whole design process of attitude controller is shown in Algorithm 4.

#### Algorithm 4

Attitude controller design process.

**Input:** desired attitude angle  $\zeta_{id} = [\phi_d, \theta_d, \psi_d]^T$ , attitude angle

$$\zeta_{i1} = [\phi, \theta, \psi]^T$$

**Output:** control torque  $\tau_i = [\tau_\phi, \tau_\theta, \tau_\psi]^T$

1: calculate LESO:  $\begin{cases} \dot{\hat{\zeta}}_{i1} = \hat{\zeta}_{i2} + \kappa_{i1} \varepsilon_{i1} \\ \dot{\hat{\zeta}}_{i2} = \hat{\zeta}_{i3} + b_i \tau_i + \kappa_{i2} \varepsilon_{i1}, \text{ where } \varepsilon_{i1} = \zeta_{i1} - \hat{\zeta}_{i1} \\ \dot{\hat{\zeta}}_{i3} = \kappa_{i3} \varepsilon_{i1} \end{cases}$

2: calculate control torque:

$$\tau_i = \frac{\lambda_{i1}(\zeta_{id} - \hat{\zeta}_{i1}) + \lambda_{i2}(\dot{\zeta}_{id} - \dot{\hat{\zeta}}_{i2}) + (\ddot{\zeta}_{id} - \ddot{\hat{\zeta}}_{i3})}{b_i}$$

**Remark 4.** If the estimation errors of the LESO converge to zero, that is  $\varepsilon_i = 0$ , the tracking errors of the attitude system are asymptotically convergent.

## 4. Simulation

In this section, trajectory tracking simulation experiments for the 12-rotor UAV under input saturation and external disturbances are carried out to illustrate the effectiveness and superiority of our proposed control algorithm. The contrast control methods for outer loop of the UAV are chosen as proportional–derivative control algorithm (Approach 4), traditional backstepping control algorithm (Approach 3), and the extended state observer–based robust dynamic surface control algorithm in Ref. [30] (Approach 2), and our proposed algorithm is marked as Approach 1. In order to make the contrast experiments more convincing, the controller parameters of the four methods are selected the same.

The physical parameters of the 12-rotor UAV are given in Table 1. The simulation lasts for 30 s. The desired reference path is a horizontal rectangle trajectory defined as follow, and the yaw angle is required to be stabilized at zero. The initial condition of the UAV is set as  $\zeta_0 = [0.5, -0.5, 0]^T$ ,  $\eta_0 = [0, 0, 0.2]^T$ , containing non-zero initial cases to further test the effectiveness of the proposed algorithm.

$$\begin{cases} x_d = \frac{4(t-5)}{5}f(t, 5,10) + 4f(t, 10,15) + \frac{4(20-t)}{5}f(t, 15,20) \\ y_d = \frac{3(t-10)}{5}f(t, 10,15) + 3f(t, 15,20) + \frac{3(25-t)}{5}f(t, 20,25) \\ z_d = \frac{3t}{5}f(t, 0,5) + 3f(t, 5,30) \end{cases}$$

where  $f(x, a, b) = \frac{\text{sign}(x-a) + \text{sign}(b-x)}{2}$ .

In order to simulate the complex real flight environment and test the robustness of the proposed control algorithm, it is assumed the external disturbances on aerodynamic force and moments are given as:  $d_x = 2 \sin(2\pi t)$ ,  $d_y$  is a step signal with the amplitude of 1 at  $t = 2s$ ,  $d_z = 1$ ,  $d_\phi$  is a ramp signal with the slope of 0.05 at  $t = 10s$ ,  $d_\theta$  is a square signal with the amplitude of 0.7, and  $d_\psi$  is a step signal with the amplitude of 0.7 at  $t = 5s$ . If the proposed algorithm makes the UAV resist every form of the external disturbances, the UAV gains strong robustness and has potential ability to cope with the changeable real flying environment. The parameter uncertainties are chosen as  $\Delta I_x = 0.1I_x$ ,  $\Delta I_y = -0.1I_y$ ,  $\Delta I_z = 0.1I_z$ . The thrust force ranging from 0N to 40N is also taken into account in the simulation to evaluate the flight character with respect to input saturation problem.

The controller gains and observer gains of the proposed algorithm are chosen as follow.

$$\begin{aligned} k_1 &= 3, k_2 = 2, l_1 = 5, l_2 = 5, \sigma = 0.8 \\ c_1 &= 0.5, c_2 = 0.78, v = 0.8 \\ \delta_{1i} &= [3,3,3], \delta_{2i} = [2,2,2] \\ \lambda_{1i} &= [2,2,2], \lambda_{2i} = [1,1,1] \\ \mu_i &= [0.5, 0.5, 0.5] \\ \omega_1 &= 75, \omega_2 = 75, \omega_3 = 20 \\ \omega_{1c} &= 25, \omega_{2c} = 25, \omega_{3c} = 7 \end{aligned}$$

The simulation results are shown in Figs. 3–10, and performance are outstanding for our proposed algorithm. Figs. 3–6 present the trajectory tracking responses under the four different control methods. For translational channels  $x$  and  $y$ , our proposed algorithm enables the UAV to approach the desired path from non-zero initial condition with the fastest speed and smallest overshoot, and for altitude channel  $z$ , the UAV also climbs the quickest under our algorithm. The above illustrates that our algorithm has the ability to improve the convergence rate and dynamic performance of the UAV. Figs. 3–6 also demonstrate the strong robustness of our algorithm since the external disturbances have little impact on the UAV. The UAV gains higher precision tracking performance than Approach 2 in Ref. [30] even without any disturbance rejection mechanism. However, for the other three contrast control methods, the UAV has slow convergence rate and poor tracking performance under external perturbations. Fig. 6 gives the horizontal rectangle trajectory tracking result in 3-D space, which further illustrates the superiority of our proposed algorithm.

Table 2 presents the integral square error (ISE) for each channel of the outer loop, which demonstrates the control performance quantitatively. From the table we can see that our proposed algorithm achieves the smallest ISE. The UAV has little tracking errors under the control of our algorithm even in the presence of external disturbances and input saturation. High precision tracking performance is ensured.

Fig. 7 shows the curves of thrust force. Since the controller parameters are selected the same, the thrust forces generated by the four control methods are basically the same. From Fig. 7 we can see that, the input saturation problem occurs in our control during the simulation experiments, while the unexpected actions caused by the saturation have been well compensated by the auxiliary system. Fig. 8 shows the curves of the state variables in auxiliary system. Apparently, the auxiliary system plays a very important role in avoiding the control performance from degradation with respect to the input saturation problem.

Fig. 9 gives the attitude regulation results, and Fig. 10 gives the lumped disturbance estimation results by LESO. Satisfactory attitude regulation performance in Fig. 9 lays a good foundation for trajectory

tracking task since the UAV is an underactuated system. We choose LADRC to design the attitude controllers due to its inherent strong robustness. The lumped disturbance including coupling, model uncertainty and external disturbance in the attitude system can be online estimated and compensated.

## 5. Conclusion

This paper investigates the finite-time trajectory tracking problem of a novel 12-rotor UAV with input saturation. Hierarchical structure is employed to design the whole control scheme. Finite-time backstepping controllers are designed for outer loop to achieve finite-time convergence property. A finite-time auxiliary system is introduced to tackle the input saturation problem without affecting the finite-time stability of the outer loop. Simple LADRC algorithm is applied to design attitude controllers in order to achieve satisfactory regulation performance under the lumped disturbances. Finally contrast simulation experiments demonstrate the perfect property of our proposed control algorithm.

By employing the finite-time control strategy, delays existing in outer loop is obviously reduced, and the system gains faster convergence rate under our control.

There is no disturbance compensation mechanism in our control algorithm, whereas the outer loop still gains strong robustness due to the exponential terms and the auxiliary system in our controller.

By introducing the finite-time auxiliary system, the controller parameter selection is relaxed to gain strong robustness, and the tradeoff between convergence rate and actuator saturation is avoided to a certain extent.

Next, we will continue to improve the property of the proposed control algorithm and real flight experiments will be carried out for the 12-rotor UAV under our method.

## Acknowledgements

This work was supported by the National Natural Science Foundation, China [granted numbers 11372309, 61304017]; the Science & Technology Development Project, Jilin, China [granted number 20150204074GX]; and Jilin University “985 Project” Engineering Bionic Sci. & Tech. Innovation Platform.

## References

- [1] Liu H, Lu G, Zhong Y. Robust LQR attitude control of a 3-DOF laboratory helicopter for aggressive maneuvers. *IEEE Trans Ind Electron* 2013;60(10):4627–36.
- [2] Hoffmann GM, Huang HM, Waslander SL, et al. Precision flight control for a multi-vehicle quadrotor helicopter testbed. *Contr Eng Pract* 2011;19(9):1023–36.
- [3] Xiong JJ, Zheng EH. Position and attitude tracking control for a quadrotor UAV. *ISA Trans* 2014;53:725–31.
- [4] Kayacan E, Maslim R. Type-2 fuzzy logic trajectory tracking control of quadrotor VTOL aircraft with elliptic membership functions. *IEEE/ASME Trans Mechatron* 2017;22(1):339–48.
- [5] Pan YN, Yang GH. Event-triggered fuzzy control for nonlinear networked control systems. *Fuzzy Set Syst* 2017;329:91–107.
- [6] Shirzadeh M, Amirkhani A, et al. An indirect adaptive neural control of a visual-based quadrotor robot for pursuing a moving target. *ISA Trans* 2015;59:290–302.
- [7] Xu ZW, Nian XH, Wang HB, Chen YS. Robust guaranteed cost tracking control of quadrotor UAV with uncertainties. *ISA Trans* 2017;99:157–65.
- [8] Mokhtari MR, Cherki B, Braham AC. Disturbance observer based hierarchical control of coaxial-rotor UAV. *ISA Trans* 2017;67:466–75.
- [9] Basri MAM. Trajectory tracking control of autonomous quadrotor helicopter using robust neural adaptive backstepping approach. *J Aero Eng* 2018;31(2). [https://doi.org/10.1061/\(ASCE\)AS.1943-5525.0000804](https://doi.org/10.1061/(ASCE)AS.1943-5525.0000804).
- [10] Zheng FY, Gong HJ, Zhen ZY. Adaptive constraint backstepping fault-tolerant control for small Carrier-based unmanned aerial vehicle with uncertain parameters. *Proc IMechE Part G: J Aero Eng* 2016;230(3):407–25.
- [11] Jia ZY, Yu JQ, et al. Integral backstepping sliding mode control for quadrotor helicopter under external uncertain disturbances. *Aero Sci Technol* 2017;68:299–307.
- [12] Zuo ZY, Mallikarjunan S. L-1 adaptive backstepping for robust trajectory tracking of UAVs. *IEEE Trans Ind Electron* 2017;64(4):2944–54.
- [13] Tan CK, Wang JL, Paw YC, Ng TY. Tracking of a moving ground target by a quadrotor using a backstepping approach based on a full state cascaded dynamics. *Appl Soft Comput* 2016;47:47–62.
- [14] Chen FY, Lei W, et al. A novel nonlinear resilient control for a quadrotor UAV via

- backstepping control and nonlinear disturbance observer. *Nonlinear Dynam* 2016;85(2):1281–95.
- [15] Jiang BY, Hu QL, Friswell MI. Fixed-time attitude control for rigid spacecraft with actuator saturation and faults. *IEEE Trans Contr Syst Technol* 2016;24(5):1892–8.
- [16] Zhu WW, Du HB, Cheng YY, Chu ZB. Hovering control for quadrotor aircraft based on finite-time control algorithm. *Nonlinear Dynam* 2017;88(4):2359–69.
- [17] Shi XN, Zhang YA, Zhou D. Almost-global finite-time trajectory tracking control for quadrotors in the exponential coordinates. *IEEE Trans Aero Electron Syst* 2017;53(1):91–100.
- [18] Xiong JJ, Zhang GB. Global fast dynamic terminal sliding mode control for a quadrotor UAV. *ISA Trans* 2017;66:233–40.
- [19] Mofid O, Mobayen S. Adaptive sliding mode control for finite-time stability of quadrotor UAVs with parametric uncertainties. *ISA Trans* 2018;72:1–14.
- [20] Wang HW, Jing YW, et al. Guaranteed cost sliding mode control for discrete time looper systems in hot strip finishing mills. *J Control Decis* 2016;3(2):151–64.
- [21] Ofodile NA, Turner MC. Decentralized approaches to antiwindup design with application to quadrotor unmanned aerial vehicles. *IEEE Trans Contr Syst Technol* 2016;24(6):1980–92.
- [22] Li SS, Wang YN, Tan JH. Adaptive and robust control of quadrotor aircrafts with input saturation. *Nonlinear Dynam* 2017;89(1):255–65.
- [23] Sarhadi P, Noei AR, Khosravi A. Adaptive integral feedback controller for pitch and yaw channels of an AUV with actuator saturations. *ISA Trans* 2016;65:284–95.
- [24] Cao N, Lynch AF. Inner-outer loop control for quadrotor UAVs with input and state constraints. *IEEE Trans Contr Syst Technol* 2016;24(5):1797–804.
- [25] Peng C, Zhao CC, Gong X, et al. Variable structure and variable coefficient proportional-integral-derivative control to prevent actuator saturation of yaw movement for a coaxial eight-rotor unmanned aerial vehicle. *Proc IMechE Part G: J Aero Eng* 2015;229(9):1661–74.
- [26] Fu CY, Tian YT, et al. Sensor faults tolerance control for a novel multi-rotor aircraft based on sliding mode control. *Proc IMechE Part G: J Aero Eng* 2018. <https://doi.org/10.1177/0954410017731590>.
- [27] Fu CY, Hong W, Lu HQ, Zhang L, Guo XJ, Tian YT. Adaptive robust backstepping attitude control for a multi-rotor unmanned aerial vehicle with time-varying output constraints. *Aero Sci Technol* 2018;78:593–603.
- [28] Fu CY, Tian YT, Zhang L, Guo XJ. Attitude control for multi-rotor aircraft with output Constraints. *Proceedings of the 6th IEEE data driven control learn syst conf (DDCLS)*. 2017. p. 247–52.
- [29] Huang X, Yan Y, Huang ZR. Finite-time control of underactuated spacecraft hovering. *Contr Eng Pract* 2017;68:46–62.
- [30] Shao XL, Liu J, et al. Robust dynamic surface trajectory tracking control for a quadrotor UAV via extended state observer. *Int J Robust Nonlinear Control* 2018;28(7):2700–19.